CrystEngComm

Accepted Manuscript

ROYAL SOCIETY OF CHEMISTRY

www.rsc.org/crystengcomm

Journal Name

COMMUNICATION

Less is more: Silicate on crystallization of hydroxyapatite in simulated body fluids

Received 00th January 20xx,
Accepted 00th January 20xx

DOI: 10.1039/x0xx00000x

www.rsc.org/

Ya-Nan Wang,[a,b] Shuqin Jiang,[b] Haihua Pan,*[a] and Ruikang Tang[b]

In this work, dual roles of silicate on crystallization of HAP in simulated body fluids were revealed. At lower concentrations of silicate (0.05-0.5 mM), it promoted the nucleation of HAP, and the less the silicate, the faster the HAP nucleation. In contrast, at higher silicate concentrations (3-8 mM), it inhibited the nucleation of HAP.

The control of crystallization was one of the key steps in biomineralization. The smart regulation strategies of biomineralization on crystallization had attracted much attention because of its inspirations on fabrications of functional materials.[1] In Biomineralization, increasing evidences supported that the transient amorphous phase played as the precursor phase for crystallization.[2] The crystal nucleation via the rearrangement of the amorphous phase is distinct from the scenario of classical nucleation. For this non-classical crystallization pathway, many distinct strategies have been found to regulate the crystallization in bio/mimetic mineralization systems.[3] These strategies include, but are not limited to, the addition of soluble inorganic ions[3a,b] and organic additives,[3c,d] being covered by lipid or surfactant,[3e,f] being confined in nano/micro-space,[3f,g] being stored in air[3e] or non-aqueous condition, [3h,i] etc.

Actually, the details of final products of biomineralization, biominerals, may shed lights on the strategy of crystallization controls. Recent experiments had found that many ions or molecules that were found in the final skeleton minerals, such as Mg^{2+}, aspartic acid, citrate and silicate etc., were turned out to play active roles in biomimetic crystallization of hydroxyapatite (HAP).[4] Among them, the enrichment of silicate in bone (100 ppm) had attracted our attention because bone had a much higher level of silicate than that in other organs, such as serum (1 ppm), liver, kidney, lung and muscle (2-10 ppm).[5] In biology, silicon is known as an essential element for normal bone growth and development.[5-6] Micro-analysis of bones showed the silicate was enriched at active calcification sites in young bones, indicating the silicate participated in bone formation during early stages.[4d, 6] However, silicon supplementation at high levels led to a reduction in bone strength, which might be caused by the decreasing plasma calcium level by the silicate.[7] Till now, the possible chemical mechanism of silicate during biomineralization remained unknown.

Silicate was known to affect the formation of minerals, such as calcium carbonate,[8] barium carbonate,[9] and calcium phosphate. [8c, 10] For example, silicates stabilized amorphous calcium carbonate and prohibited its crystallization.[8a] Silicate was alternatively co-precipitated with barium carbonate.[9b] Silicate induced the precipitation of HAP.[11] However, its regulation mechanism on crystallization was not revealed, which was a fundamental question to biomineralization. To this end, we quantitatively evaluated the effect of silicate on kinetics of HAP nucleation in simulated body fluids (SBF) with varies amount of silicate, and discovered dual roles and dose dependent effects of silicate on HAP crystallization.

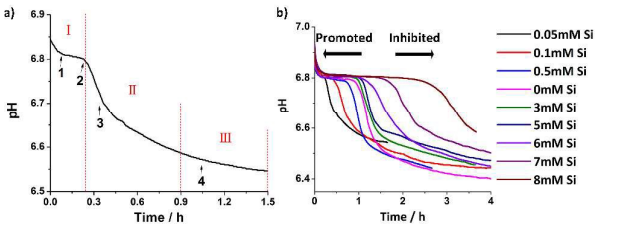

Fig. 1 a) Representative pH curves of HAP crystallization under SBF in the presence of 0.05 mM silicate. The crystallization process could be divided into three stages, named stage I, II, III. b) Dual roles and dose dependent effects of silicate on HAP nucleation.

The crystallization of HAP in SBF solutions were monitored by a pH meter because HAP formation was accompanied by a significant drop in solution pH (see eq. 1).[12]

$$3Ca_3(PO_4)_2(s) + Ca^{2+} + 2H_2O \rightarrow 2Ca_5(PO_4)_3(OH)(s) + 2H^+ \quad (1)$$

[a] Qiushi Academy for Advanced Studies, Zhejiang University, Hangzhou, Zhejiang, China. 310027 E-mail: panhh@zju.edu.cn
[b] Department of Chemistry, Zhejiang University, Hangzhou, Zhejiang, China. 310027 E-mail: rtang@zju.edu.cn

† Electronic Supplementary Information (ESI) available: Experimental details and FTIR, XRD, TEM, XPS, Zeta potential characterizations and Measurement of S_a. See DOI: 10.1039/x0xx00000x

By a pH curve, HAP crystallization processes could be divided into three stages (Fig. 1a). [12c, 13] Stage I: the pH reached at designated pH after the mixing of calcium solutions and phosphate solutions, and then kept relative stable. Stage II: the pH dropped faster as the occurrence of HAP crystallization. Stage III: the pH gradually levelled off as HAP ripening. Before the onset of HAP nucleation, there was a lag time, which could be quantitatively determined by the interception of stage I and II. The lag time is an indication for the stability of ACP. The more stable the ACP, the longer the lag time. And in this work, the nucleation rate, J_N, was expressed as follows:

$$J_N=1/(tV) \quad (2)$$

in which t was the lag time and V was the volume of the system, which was 10 mL in this work.

Two opposite effects of silicate on nucleation kinetics of HAP were observed (representative pH curves were showed in Fig. 1b). Promotion effect: lower concentration of silicate (0.05-0.5mM) shorten the lag time and accelerated HAP nucleation. Unexpectedly, the lower the concentration of silicate, the shorter the lifetime of ACP (the faster the HAP nucleation). Inhibition effect: higher concentration of silicate (3-8 mM) prolonged the lag time and thus inhibited the nucleation of HAP. The inhibition effect increased with increasing silicate concentration.

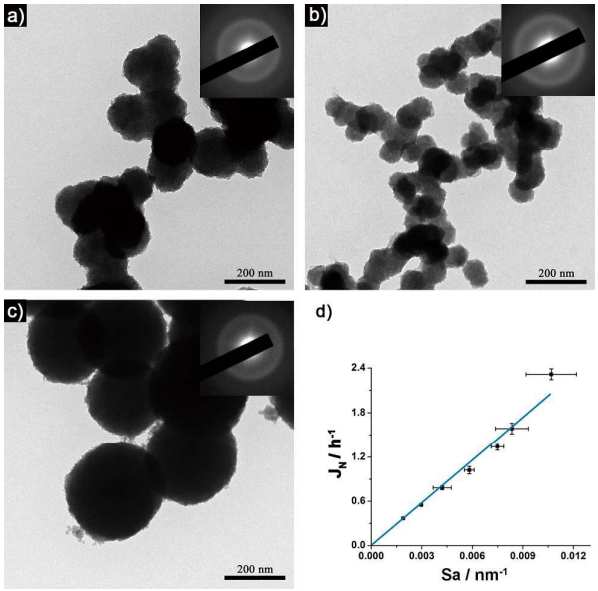

Fig. 2 TEM images of ACP particles and the electron diffractions (inset) at 5 min. (a) control group (0 mM silicate), the diameter of ACP particles were about 100 nm; (b) 0.05 mM silicate, the diameter was about 50 nm; (c) 8 mM silicate, the diameter was about 200 nm. (d) The HAP nucleation rate was correlated with the specific surface area of ACP.

In the classical understanding of nucleation, the nucleation kinetics is primarily affected by the supersaturation and the interfacial energy of nuclei.[14] In principle, higher supersaturation and lower interfacial energy give shorter induction time. In this work, the chelation of dilute silicate (0.05 mM) with calcium can be neglected. So, the introduction of silicate had less effect on the supersaturation of HAP. Even if we take the slight decreasing of supersaturation (because of the chelation of dilute silicate) into account, in principle, this will slightly inhibit HAP nucleation. But this prediction contradicts the fact that dilute silicate actually promotes HAP nucleation (Fig. 1b). In this regard, the change of nucleation kinetics cannot be explained by the alternation of supersaturation. Therefore, we turned to the factor of interfacial tension of HAP nuclei, which might be reduced in the presence of silicate. In principle, the more the additive, the lower the interfacial energy. However in this work, less silicate promoted HAP nucleation more (indicating lower interfacial energy). These contradictions cannot be well explained by the classical nucleation theory.

Based upon our previous understandings on the kinetics of ACP-mediated HAP nucleation in simulated body fluids, [12c, 13] HAP nucleation rate was correlated with the state of ACP (eg. the size, surface area, and additive adsorption). We postulated that silicate might affect the state of ACP, which was later corroborated by our experiments as given below.

Firstly, we confirmed that in our system, the crystallization of HAP was intermediated by ACP precursor. At designated time intervals (marked in Fig. 1a by numbers 1 - 4), the phase of slurry samples were determined by TEM, FTIR and XRD. In the presence of 0.05 mM silicate, ACPs formed at stage I (at 5 min) (see TEM images in Fig. S1a). At the phase transition time point (at 15 min, Fig. S1b), HAP platelets fingering out of ACP surface were frequently observed, which was also reported previously.[4b, 12c, 15] With the evolving (stage II, 20 min, Fig. S1c), more HAP crystallites were grown by the consumption of ACPs, and finally (at stage III, 60 min, Fig. S1d), ACPs were completely transformed to HAP. SAED patterns (Fig. S1e-h) showed that bright diffraction rings appeared out of diffusive diffractions, supporting the nucleation of HAP from ACP. FTIR spectra (Fig. S2) showed the gradual splitting of absorption bands at about 1055 cm^{-1} (phosphate ν_3 vibrations) and 570 cm^{-1} (phosphate ν_4 bending), supporting the transformation of ACP to HAP.[16] And XRD patterns (Fig. S3) also confirmed the phase evolving from ACP to HAP. Similar crystallization pathway had been found for higher concentration of silicate (8 mM) (Fig. S4) and the other systems (not given here).

Secondary, we checked the state of ACP. TEM images showed that the size of ACP was distinct in the presence of silicate (Fig. 2/S5). In the absence of silicate (control group), ACP particles had a mean diameter of 100±12 nm, and in the presence of small amount of silicate, the diameter of ACP particles became smaller (they were 56±6, 70±8 and 90±5 nm for 0.05, 0.1 and 0.5 mM silicate, respectively) (see image analysis in ESI, Fig. S9-S11). But they became larger under high concentration of silicate (130±12, 160±9 and 210±15 nm for 6, 7 and 8 mM silicate, respectively) (Fig. S13-S15). By the quantitative analysis of TEM images, the specific surface area of ACPs ($S_a=A_{ACP}/V_{ACP}$, where A_{ACP} was the total surface area of ACP, V_{ACP} was the total volume of ACPs) was estimated (see ESI). We found that the nucleation rate was correlated with the surface area of ACPs (Fig. 2d), which fit the surface nucleation model.[12c,13] We concluded that the dual roles of silicate on HAP nucleation were correlated with the state of ACP (different size/surface area).

To answer how silicate affected the size of ACPs and why their effects were dose-dependent, we need to know the participation of silicate during ACP formation. First of all, we found that silicate was co-precipitated with ACP by EDX analysis (at 5-10 min, Fig. 3c/S6). FTIR spectra (Fig. S2/S4e) also

showed the presence of bending absorption of Si-O-Si (471cm^{-1}) [10b] in ACPs. The quantitative EDX (by SEM) analysis of ACP precipitates indicated that the Si/Ca atomic ratio was about 2.4% (Fig. S6). For higher concentration of silicate (8 mM), the Si/Ca ratio increased to 21%. The surface analysis of initial ACPs (at 10 min, 8 mM silicate) by XPS spectra (it could only detect outermost 10 nm surface material) showed a strong signal of polysilicate (Fig. S7), supporting the presence of silicate on the surface of ACP. After the decalcification of ACP by excessive amount of EDTA (2 mL 500 mM), the thin shell of polysilicate can be observed (Fig. 3b). The EDX analysis showed that the major element was Si (Fig. 3d).

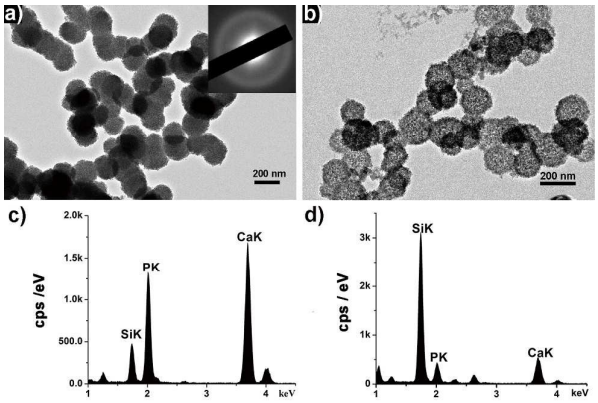

Fig. 3 TEM images (a, b) and EDX analysis (c, d) of ACP precipitations (10 min, in the presence of 8 mM silicate) (a, c) and decalcified precipitates (b, d). a) ACP particles; b) after decalcification, a silicate shell was revealed; c) ACP contains Ca, P and Si; d) after decalcification, the major element is Si.

The thickness of polysilicate shell became thicker at later stage of ACPs. At about 40 min, the polysilicate shell could be directly observed by HRTEM (Fig. 4). The silica shell had a lower electron density than that of amorphous calcium mineral.[8a] In our observations, the polysilicate shell was porous (Fig. 4). The thickness of polysilicate shell reached at about 10±4 nm for longer incubation time (70 min) (Fig. 4b, e).

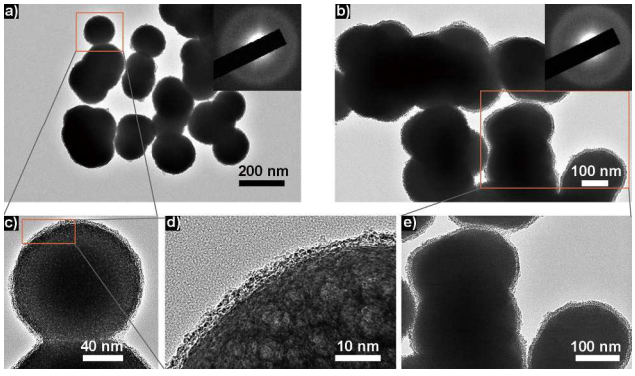

Fig. 4 HRTEM images of polysilicate/ACP core-shell structure at higher silicate concentrations (8 mM) at 40 min (a/c/d) and 70 min (b/e).

It had been reported that silicate could be polymerized and be precipitated on the surface of amorphous calcium carbonate.[8a] The similar mechanism could be applied here to explain the formation of core-shell structure (6-8 mM silicate was equivalent to 360-480 ppm SiO_2, which was close to previous work of calcium carbonate).[8a] Accompanied with ACP precipitation as the mixing of calcium and phosphate solutions, proton was released (cf. eq. 1). So, as the increasing of the local pH near ACP surface, the local supersaturation of silicate was increased, which triggered the polymerization of silicate.[17] The deconvolution of the FTIR spectra of the ACP/silica minerals (8 mM silicate) showed representative absorbance peaks of silica (marked in Fig. S16). It turned out that the silica contained both cyclic (1198 cm^{-1}), linear and less cross-linked structure (1157 cm^{-1}).[18] The Si-O-Si stretching vibration band at 1080 and 1055 cm^{-1} were shifted to lower wavenumber of 1072 and 1023 cm^{-1}, respectively, indicating that the silica was porous,[18] which can be observed in TEM images (Fig. 3b, 4) and . With the aging of mineral, the absorbance band at 950 cm^{-1} (Si-O$^-$) increased its intensity and the band at 980 cm^{-1} (Si-OH) decreased its intensity (Fig. S16), which was similar to the effect of decreasing pH on a silica gel.[18] This is coincided with the fact that pH is decreasing as the mineralization (Fig. 1). The initially formed polysilicates might be loose and flexible, and as the condensation of polysilicate, they would shrink to reduce the total surface area and enhance the cross-linking. This shrinking process dragged nearby loose-aggregated ACPs and led to the merging of these ACPs (Fig. 4). As a result, the size of primary particles was increased in the presence of high concentration of silicate (cf. Fig. 2). As the merging, the outer polysilicate shell became thicker (Fig. 4) and the total surface area of ACP was reduced (Fig. 2).

In contrast, for diluted silicate solutions (0.05-0.5 mM, equivalent to 3-30 ppm SiO_2), the size of ACPs became even smaller than that of control experiments (without silicate) (cf.Fig.2). In addition, the ACPs size became smaller as the decreasing of silicate concentration. In solution chemistry of silicate, 3-30 ppm silicate was still undersaturated for amorphous silica.[17] So, the spontaneous precipitation or polymerization of silicate would not happen for these solutions. The primary species of silicate in solutions were silicate monomers or oligomers as confirmed by dynamic light scattering (DLS) experiments (Fig. 5a). The monomers or oligomers were charged species in solution as the deprotonation of silicate (eq. 3-4)[19], which was confirmed by the zeta potential measurements (Fig. 5b).

$$Si(OH)_4 + OH^- \rightarrow SiO(OH)^{3-} + H_2O \quad (3)$$

$$SiO(OH)^{3-} + OH^- \rightarrow SiO_2(OH)_2^{2-} + H_2O \quad (4)$$

These charged silicate species could attract calcium ions in solution and played as the heterogeneous nucleation centre for ACPs. With the precipitation of ACPs, silicate was included as well (Fig. S2, S6). In this way, silicate would be enriched in mineral during the precipitation of ACP, which can explain the high level of silicate at mineralization front of growing bone.[6] DLS measurement confirmed that the higher the concentration of silicate, the larger the silicate oligomer, but the less negative the zeta potential (Fig. 5). Clearly, the nucleation of ACP was more readily for silicate oligomers with more negative zeta potential (higher charge density), which was abundant for silicate solutions at lower concentrations. So, more ACPs nuclei would be induced by dilute silicate solutions, and the final size of ACP particles would be smaller because the same amount of calcium phosphate nutrients were shared by more nuclei. This can explain why smaller ACPs were formed in dilute silicate

solutions (cf. Fig. 2, Fig. S5). Note that in physiological fluid, the level of silicate is at the level of ppm, which is a dilute silicate solution. According to this work, this silicate will promote HAP mineralization. These findings will help us on the understanding of the essential role of silicate in biomineralization.

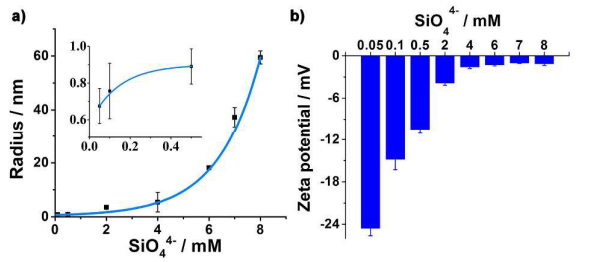

Fig. 5 a) DLS analysis of silicate particle size (hydrodynamic radius) under various concentrations. b) Zeta potential of silicate particles.

In summary, dual roles of silicate on ACP-mediated HAP nucleation were revealed, which was dependent upon the state of silicate. Undersaturated silicate solutions (0.05-0.5 mM) contained charged silicate monomer and oligomers, which played as heterogeneous nucleation centre for ACPs. As a result, smaller ACP particles with larger surface area were formed, which nucleated HAP faster. In contrast, for high concentration of silicate (3-8 mM), silicates were polymerized and precipitated on ACP surface, which led to the merging of nearby ACPs and produced larger ACPs (with smaller surface area) with a shell of polysilicate. In this condition, nucleation of HAP was retarded. This dose dependent effect of silicate on HAP nucleation enriched our understanding on chemical functions of silicate during bone formation.

Notes and references

‡ This work is supported by the Fundamental Research Funds for the Central Universities, National Natural Science Foundation of China (20973152).

1 (a) S. V. Dorozhkin and M. Epple, *Angew. Chem. Int. Ed.* 2002, **41**, 3130; (b) F. C. M. Driessens, *Bull. Soc. Chim. Belg.* 1980, **89**, 663; (c) M. Goldberg, A. B. Kulkarni, M. Young and A. Boskey, *Front. Biosci., Elite Ed.* 2011, **3**, 711; (d) S. Weiner and H. D. Wagner, *Annu. Rev. Mater. Sci.* 1998, **28**, 271.

2 (a) J. D. Termine and A. S. Posner, *Science* 1966, **153**, 1523; (b) E. Beniash, J. Aizenberg, L. Addadi and S. Weiner, *Proc. R. Soc. B-Biol. Sci.* 1997, **264**, 461; (c) Y. Politi, T. Arad, E. Klein, S. Weiner and L. Addadi, *Science* 2004, **306**, 1161; (d) J. Mahamid, B. Aichmayer, E. Shimoni, R. Ziblat, C. Li, S. Siegel, O. Paris, P. Fratzl, S. Weiner and L. Addadi, *Proc. Natl. Acad. Sci. U. S. A.*, 2010, **107**, 6316.

3 (a) J. Aizenberg, G. Lambert, S. Weiner and L. Addadi, J. Am. Chem. Soc. 2002, 124, 32; (b) E. Loste, R. M. Wilson, R. Seshadri and F. C. Meldrum, *J. Cryst. Growth* 2003, 254, 206; (c) H. Cölfen and L. Qi, *Chem. Eur. J.* 2001, **7**, 106; (d) A. W. Xu, Y. Ma and H. Cölfen, *J. Mater. Chem.* 2007, **17**, 415; (e) K. Lee, Kyubock, W. Wagermaier, A. Masic, K. P. Kommareddy, M. Bennet, I. Manjubala, S.-W. Lee, S. B. Park, H. Cölfen and P. Fratzl, *Nat. Commun.* 2012, **3**, 725. (f) C. C. Tester, R. E. Brock, C. H. Wu, M. R. Krejci, S. Weigand and D. Joester, *CrystEngComm*, 2011, 13, 3975; (g) E. Loste, R. J. Park, J. Warren and F. C. Meldrum, *Adv. Funct. Mater.* 2004, **14**, 1211; (h) H. S. Lee, T. H. Ha and K. Kim, *Mater. Chem. Phys.* 2005, **93**, 376; (i) X. R. Xu, A. H. Cai, R. Liu, H. H. Pan, R. K. Tang and K. Cho, *J. Cryst. Growth* 2008, **310**, 3779.

4 (a) B. Cantaert, E. Beniash and F. C. Meldrum, *J. Mater. Chem. B*, 2013, **1**, 6586; (b) H. C. Ding, H. H. Pan, X. R. Xu and R. K. Tang, *Cryst. Growth Des.* 2014, **14**, 763; (c) Y. Y. Hu, A. Rawal and K. Schmidt-Rohr, *Proc. Natl. Acad. Sci. U. S. A.* 2010, **107**, 22425; (d) Z. Y. Qiu, I. S. Noh and S. M. Zhang, *Front. Mater. Sci.* 2013, **7**, 40.

5 A. M. Pietak, J. W. Reid, M. J. Stott and M. Sayer, *Biomaterials* 2007, **28**, 4023.

6 E. M. Carlisle, *Science* 1970, **167**, 279.

7 (a) C. T. Price, K. J. Koval and J. R. Langford, *Int. J. Endocrinol* 2013, **2013**, 316783; (b) H. Kayongo-Male and J. L. Julson, *Biol. Trace Elem. Res.* 2008, **123**, 191.

8 (a) M. Kellermeier, E. M. Garcia, F. Glaab, R. Klein, M. Drechsler, R. Rachel, J. M. Garcia Ruiz and W. Kunz, *J. Am. Chem. Soc.* 2010, **132**, 17859; (b) G. J. Stockmann, D. W. Boenisch, N. Bovet, S. R. Gislason and E. H. Oelkers, *Geochim. Cosmochim. Acta* 2014, **135**, 231; (c) M. Kellermeier, D. Gebauer, E. M. Garcia, M. Drechsler, Y. Talmon, L. Kienle, H. Cölfen, J. M. Garcia-Ruiz and W. Kunz, *Adv. Funct. Mater* 2012, **22**, 4301.

9 (a) G. Rajaretnam and H. B. Spitz, *Health Phys.* 2000, **78**, 191; (b) J. Eiblmeier, U. Schuermann, L. Kienle, D. Gebauer, W. Kunz and M. Kellermeier, *Nanoscale* 2014, **6**, 14939.

10 (a) D. Arcos, J. R. Carvajal and M. V. Regi, *Chem. Mater.* 2004, **16**, 2300; (b) M. S. Sadjadi, H. R. Ebrahimi, M. Meskinfam and K. Zare, *Mater. Chem. Phys.* 2011, **130**, 67.

11 Y. Tanizawa and T. Suzuki, *J. Chem. Soc., Faraday Trans.* 1995, **91**, 3499.

12 (a) P. Koutsoukos, Z. Amjad, M. B. Tomson and G. H. Nancollas, *J. Am. Chem. Soc*. 1980, **102**, 1553; (b) J. Christoffersen, M. R. Christoffersen, W. Kibalczyc and F. A. Andersen, *J. Cryst. Growth* 1989, **94**, 767; (c) S. Jiang, Y. Chen, H. Pan, Y. J. Zhang and R. Tang, *Phys. Chem. Chem. Phys.* 2013, **15**, 12530.

13 S. Jiang, H. Pan, Y. Chen, X. Xu and R. Tang, *Faraday Discuss.* 2015, **179**, 451.

14 P. G. Vekilov, *Nanoscale* 2010, **2**, 2346.

15 Y. Chen, W. J. Gu, H. H. Pan, S. Q. Jiang and R. K. Tang, *CrystEngComm*, 2014, **16**, 1864.

16 H. A. Lowenstam and S. Weiner, *Science* 1985, **227**, 51.

17 R. K. Iler, *The Chemistry of Silica. Solubility, polymerization, Colloid and Surface Properties, and Biochemistry*, John Wiley and Sons, New York, **1979**.

18 M. Iafisco, M. Marchetti, J. G. Morales, M. A. Hernandez-Hernandez, J. M. G. Ruiz and N. Roveri, *Cryst. Growth Des.* 2009, **9**, 4912.

19 C. E. White, J. L. Provis, G. J. Kearley, D. P. Riley and J. S. J. van Deventer, *Dalton Trans.* 2011, **40**, 1348.

Journal Name

COMMUNICATION

Less is more: Silicate on crystallization of hydroxyapatite in simulated body fluids

Ya-Nan Wang,[a,b] Shuqin Jiang,[b] Haihua Pan,*[a] and Ruikang Tang[b]

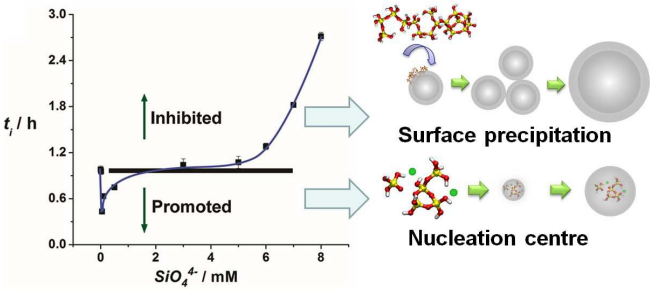

Dilute silicate (0.05-0.5mM) promoted the nucleation of hydroxyapatite (HAP) in simulate body fluids, while higher level of silicate (3-8mM) inhibited it.